FUDMA Journal of Engineering and Technology
ISSN: 3092-9385
https://fjet.fudutsinma.edu.ng/index.php/fjet/
Volume 2, Issue 2, 2026, 350-361

Snail Shell-Clay Ceramic Composites as Sustainable Raw Materials for High-Voltage Insulators

Ferguson H. TOBINS[1*], Ishiaka S. ARUDI[2], Abdulhakeem H. NURUDEEN[3]

[1*]Trinity College Dublin, The University of Dublin. Dublin, Ireland
[2]department of Mechanical Engineering, University of Abuja, Abuja, Nigeria

[1*]fergusontobins@gmail.com, [2]shuaibu.ishiaka@uniabuja.edu.ng, [3]hassan.abdulhakeem@uniabuja.edu.ng

Abstract
This study investigates the potential of Giant African Land Snail (GALS) shell–clay ceramic composites as raw materials for high-voltage insulators. The primary aim was to evaluate the influence of firing temperature on the physical properties of these composites and determine their suitability for electrical applications. Crushed GALS shell particles (63 µm and 75 µm) were blended with clay (<120 µm) in varying ratios to produce composites designated 631090, 632080, 751090, and 752080, alongside a pure clay control (C100). Samples were fired at 1160°C, 1180°C, and 1200°C. Physical properties, including shrinkage, water absorption, porosity, and bulk density, were assessed following ASTM standards (1985a). Dry shrinkage remained within acceptable limits (3.6%), while fired shrinkage increased with temperature. Notably, sample 752080 exhibited reduced shrinkage (4.89% at 1200°C) compared to the control (5.93%), indicating that snail shell inclusions constrained contraction. Water absorption and porosity decreased with increasing firing temperature, while density improved, particularly in shell-containing composites. Above 1180°C, partial fusion and glassy phase formation enhanced densification and mechanical strength. Firing at 1200°C produced optimal results, yielding composites with reduced porosity, improved density, and controlled shrinkage. These findings demonstrate that GALS shell–clay ceramics are promising candidates for the manufacture of durable high-voltage insulators, effectively bridging biomimetic inspiration with industrial application.

Keywords: *Snail shell, ceramic composites, firing temperature, porosity, water absorption, bulk density, sustainable materials.*

1.0 Introduction

Snails provide a unique biological record through their shells, which persist as measurable indicators of individual existence even after death [1]. Among them, the Giant African Land Snail (GALS) (*Achatina fulica*), belonging to the family Achatinidae within the class Gastropoda and phylum Mollusca, is distinguished by its considerable size, reaching up to 20 cm in length and 12 cm in diameter [2]. The calcareous composition of its shell has attracted scientific interest across disciplines, including biology, chemistry, engineering, and medicine [3]. In the context of materials science, the rapid pace of technological advancement necessitates the exploration of novel composites that combine properties beyond those of their individual constituents. The present study builds upon this imperative by investigating the potential of GALS shown in Figure 1, in combination with clay, as a basis for engineering materials with enhanced performance characteristics.

Figure 1: Giant African Snail Shell

Research on snail shells Due to their widespread availability, minimal cost, and substantial calcium carbonate ($CaCO_3$) content, snail shells present valuable prospects for incorporation into sustainable material systems. In light of the rising volumes of waste associated with population expansion and industrialization, the utilization of snail shells represents more than a disposal solution, it constitutes a strategic avenue for environmentally conscious construction practices. Transforming this underexploited resource can alleviate landfill pressures, conserve finite raw materials, and reinforce circular economy principles within the building industry. Applications of snail shell waste include its integration into construction composites, functioning as stabilizing agents, alkali activators, and partial substitutes for cementitious binders [4], [5]. A recurring theme in these investigations is the evaluation of clay-based ceramics under varying firing temperatures to determine their structural, mechanical, and thermal properties. Such studies are particularly relevant to the development of ceramic matrix composites for electrical

insulation, where performance depends on achieving high dielectric strength, mechanical robustness, and resistance to environmental degradation, including humid and corrosive conditions [6], [7]

Ceramic insulators are essentially ceramic matrix composites, and their properties are strongly influenced by phase transformations during firing [8]. The addition of carbonate to iron-rich kaolinite and observed the formation of mullite, cristobalite, and hematite, with gehlenite and anorthite appearing above 1150°C. Between 1150°C and 1200°C, densification increased, reducing porosity and enhancing flexural strength. However, beyond 1200°C, excessive glassy phase formation led to fragility, reduced strength, and diminished porosity. Similarly, [9] analyzed the mineralogical and microstructural changes in ceramics fired between 950°C and 1350°C. Their findings highlighted the disappearance of γ-Al_2O_3 spinel above 1250°C, a progressive increase in cristobalite, and relatively stable mullite content between 1150°C and 1350°C, all of which influenced thermal conductivity and mechanical stability.

[11], [12] provided further insight into calcareous clays, demonstrating that abundant carbonate content promotes high porosity and lowers vitrification onset to 700–800°C compared to Ca-poor clays. However, vitrification was limited at higher temperatures due to crystallization of Ca- and Mg-silicates following phyllosilicate decomposition. These findings underscore the complex interplay between mineralogy, firing temperature, and composite performance.

Collectively, these studies establish a foundation for exploring alternative biomaterials such as snail shells in ceramic composites. Their calcareous composition and structural resilience suggest potential for enhancing densification, reducing porosity, and improving mechanical strength, thereby aligning with the stringent requirements of high-voltage ceramic insulators.

Kaolin, a clay mineral whose principal constituent is kaolinite [$Al_2Si_2O_5(OH)_4$], has been extensively studied for its structural and microstructural transformations under thermal treatment [13] reported that firing kaolin at 1200°C initiates cristobalite crystallization from amorphous silica, accompanied by significant mullite formation, a finding consistent with earlier works [14], [15]. The dissolution of Al_2O_3 into the liquid phase during firing further promotes mullite crystal growth, as noted by [14], [16], [17], [18]. At temperatures exceeding 1400°C, cristobalite vitrification represents the final transformation stage.

[19] investigated composites of mullite and corundum prepared by reaction sintering of kaolinite (75 wt.%) and calcined alumina (25 wt.%). Their results demonstrated limited densification at 1400°C, with alumina remaining largely inert, while primary mullite evolved from kaolinite reactions. At 1600°C, however, a dense microstructure was achieved, yielding a flexural strength of 45 MPa compared to 15 MPa at lower temperatures. Mullite's stability at high temperatures, coupled with its low thermal expansion, high melting point, and excellent dielectric properties, underscores its suitability for thermal and electrical insulation applications [20].

Complementary studies have examined quartz transformations and mullite growth in kaolin ceramics [21], [22], [23], [24], the studies have shown mullite formation beginning at 1050–1100°C, with needle-shaped grains developing at higher temperatures up to 1600°C. These transformations highlight the critical role of firing temperature in determining ceramic microstructure and mechanical performance. [24] Extended this research to practical applications by fabricating porcelain insulators from Ethiopian raw materials. Their systematic characterization and firing experiments (1000–1300°C) revealed correlations between firing temperature and key properties such as porosity, density, dielectric strength, and microstructure, reinforcing the importance of thermal processing in optimizing ceramics for electrical insulation.

Firing clay-based ceramics at controlled temperatures induces phase transformations that significantly alter their physical, chemical, electrical, and mechanical properties. Such transformations are critical in tailoring ceramics for advanced engineering applications, particularly in electrical insulation systems where performance depends on optimized microstructural and densification behavior.

Another study [25] presents a systematic investigation into the incorporation of Giant African Land Snail (GALS) shell inclusions within clay-based ceramic composites, with particular emphasis on their suitability for high-voltage electrical insulation. The study sought to evaluate how bio-derived $CaCO_3$ from snail shells influences the mechanical, physical, and dielectric properties of clay composites when subjected to controlled firing conditions, especially at 1200 °C. it contributes to the growing body of literature on bio-derived ceramic composites, demonstrating that 1200 °C firing is the critical threshold for achieving the balance of mechanical strength, dielectric reliability, and eco-sustainability. It positions GALS shell–clay composites as promising candidates for next-generation high-voltage insulators, while simultaneously advancing sustainable materials engineering. El masloumi [26] investigates the incorporation of snail shell waste into N'Fis river clay deposits as a sustainable pathway for fired brick production. Motivated by global clay shortages and environmental concerns, the research systematically evaluates composites containing varying proportions of snail shells (0–100 wt%) fired at 900, 1000, and 1200 °C. Comprehensive analyses including particle size distribution, carbonate content, XRF, XRD, SEM, FTIR, LOI, and Atterberg limits were employed to characterize the materials. Mineralogical results revealed that the N'Fis deposit comprises ~40% clay minerals (illite, kaolinite, chlorite, smectite), 24% quartz,

Received: 28/08/2026; Revised: 29/08/2026; Accepted: 31/08/2026; Published: 31/08/2026

20% feldspar, and 15% carbonates, confirming its suitability for brick manufacture. The addition of snail shells, rich in $CaCO_3$, increased porosity and weight loss during firing, thereby reducing mechanical strength. Compressive strength declined from 24.6 MPa (pure deposit) to 14.5 MPa (50 wt% shells), yet remained above international standards (EN 772-1: 10 MPa; Moroccan norms: 4 MPa). Conversely, thermal conductivity decreased markedly (0.77 → 0.20 W/m·K), enhancing insulation, while bulk density reduction produced lightweight bricks.

The findings highlight a performance trade-off: improved thermal efficiency and reduced density at the expense of strength, though still within acceptable limits. Overall, the combined use of river deposits and snail shells offers an eco-efficient, economical, and environmentally responsible solution for producing lightweight, insulating fired clay bricks, contributing to sustainable construction and waste valorization investigates the incorporation of snail shell waste into N'Fis river clay deposits as a sustainable pathway for fired brick production. Motivated by global clay shortages and environmental concerns, the research systematically evaluates composites containing varying proportions of snail shells (0–100 wt%) fired at 900, 1000, and 1200 °C. Comprehensive analyses—including particle size distribution, carbonate content, XRF, XRD, SEM, FTIR, LOI, and Atterberg limits—were employed to characterize the materials. Mineralogical results revealed that the N'Fis deposit comprises ~40% clay minerals (illite, kaolinite, chlorite, smectite), 24% quartz, 20% feldspar, and 15% carbonates, confirming its suitability for brick manufacture.

The addition of snail shells, rich in $CaCO_3$, increased porosity and weight loss during firing, thereby reducing mechanical strength. Compressive strength declined from 24.6 MPa (pure deposit) to 14.5 MPa (50 wt% shells), yet remained above international standards (EN 772-1: 10 MPa; Moroccan norms: 4 MPa). Conversely, thermal conductivity decreased markedly (0.77 → 0.20 W/m·K), enhancing insulation, while bulk density reduction produced lightweight bricks. The findings highlight a performance trade-off: improved thermal efficiency and reduced density at the expense of strength, though still within acceptable limits. Overall, the combined use of river deposits and snail shells offers an eco-efficient, economical, and environmentally responsible solution for producing lightweight, insulating fired clay bricks, contributing to sustainable construction and waste valorization.

The present study investigates the influence of firing temperature on the physical properties specifically shrinkage, water absorption, porosity, and bulk density of ceramic matrix composites derived from mixtures of crushed (GALS) shells and clay at varying ratios. The objective was to evaluate the suitability of these bio-derived composites as potential raw materials for the fabrication of high-voltage insulators. By systematically analyzing the thermal response of GALS–clay composites under different firing regimes, this work seeks to establish correlations between processing conditions and property development, thereby contributing to the broader effort of integrating biomimetic resources into functional ceramic technologies.

2.0 Materials and Methods/Methodology

The primary raw materials employed in this study were snail shells and clay. The snail shells were obtained from the GALS (*Achatina fulica*), a species widely distributed in Southern Nigeria. Specifically, shells were collected from the Kugbo Clan and Port Harcourt areas of Rivers State. The source of these shells was predominantly post-consumer waste, gathered from refuse dumps and restaurant discards. This approach not only ensured the availability of sufficient quantities of shells but also aligned with sustainable practices by valorizing biological waste streams. The calcareous composition of the shells, rich in calcium carbonate, renders them suitable for incorporation into ceramic composites. The clay used in this study was locally sourced and processed to particle sizes below 120 μm, ensuring homogeneity in mixing and compatibility with the crushed snail shell particles. Together, these materials formed the basis for the experimental ceramic matrix composites investigated for potential application in high-voltage insulators shown in Figure 2.

Figure 2: GALS dried under the sun

Received: 28/08/2026; Revised: 29/08/2026; Accepted: 31/08/2026; Published: 31/08/2026

The clay used for this study was fireclay, supplied by "Goodwins": BUILD & DIY PRODUCTS" in Dublin as DINEEN CLAY MIX. It is a combination of shale and fireclay and has the following typical analysis (Table 1) as supplied by BUILD & DIY PRODUCTS'

Table 1: The analysis of the Dublin clay as supplied by

S/N	Clay mix constituents	Percentage (%)
1	Al_2O_3	25
2	SiO_2	63
3	Fe_2O_3	7.5
4	K_20	2.5
5	Na_2O	1.4
6	MgO	0.4
7	CaO	0.2
Total		100

The clay employed in this work contained 12% fired grog of identical chemical composition. Fire clay, a refractory material composed predominantly of hydrous aluminum silicates with or without free silica, was selected due to its high thermal resistance. It is capable of withstanding minimum temperatures of 1515°C and exhibits fusion points exceeding 1600°C, making it particularly suitable for ceramic applications requiring durability under extreme thermal conditions. The clay was processed to particle sizes below 120 μm to ensure homogeneity in mixing with the snail shell powders.

Together, these materials provided a composite system designed to exploit the calcareous nature of the snail shells and the refractory properties of fire clay, with the aim of producing ceramic matrix composites suitable for high-voltage insulator applications.

2.1.1 Sample Preparation

Rectangular test specimens were prepared using a mould of dimensions 90 mm × 14 mm × 7 mm, in accordance with ASTM D3039 [12] and ASTM D790-93 [27] standards. The crushed GALS shells were mixed with clay at varying ratios to produce ceramic matrix composites. For instance, to obtain a mixture containing 10% GALS and 90% clay (10:90), 10 g of snail shell particles (63 μm) were combined with 90 g of clay particles (<120 μm). Approximately 20–25 ml of water was added to the dry mixture to achieve plasticity and ensure uniform dispersion of the powders. The mixture was thoroughly homogenized and subsequently packed into the mould by ramming.

The moulded specimens were allowed to dry under ambient conditions for 12 hours to remove excess moisture and achieve sufficient green strength prior to firing. This procedure was repeated for all designated mixing ratios and particle sizes to produce consistent test samples for subsequent thermal treatment and property evaluation.

The following samples in the Table 2 were produced and fired at 1160°C, 1180°C, and 1200°C separately after drying at 200°C for 2 hours.

Table 2: Sample descriptions

S/N	Sample	Description	Temp Fired (°C)
1	C1001160	100%wt clay	1160
2	C1001180	100%wt clay	1180
3	C1001200	100%wt clay	1200
4	6310901160	(63 μm, 10%wt GALSs and 90%wt clay).	1160
5	6310901180	(63 μm, 10%wt GALSs and 90%wt clay).	1180
6	6310901200	(63 μm, 10%wt GALSs and 90%wt clay).	1200
7	6320801160	(63 μm, 20%wt GALSs and80%wt clay).	1160
8	6320801180	(63 μm, 20%wt GALSs and 80%wt clay).	1180
9	6320801200	(63 μm, 20%wt GALSs and 80%wt clay).	1200
10	7510901160	(75 μm, 10%wt GALSs and 90%wt clay)	1160
11	7510901180	(75 μm, 10%wt GALSs and 90%wt clay)	1180
12	7510901200	(75 μm, 10%wt GALSs and 90%wt clay)	1200
13	7520801160	(75 μm, 20%wt GALSs and 80%wt clay)	1160
14	7520801180	(75 μm, 20%wt GALSs and 80%wt clay)	1180
15	7520801200	(75 μm, 20%wt GALSs and 80%wt clay)	1200

Received: 28/08/2026; Revised: 29/08/2026; Accepted: 31/08/2026; Published: 31/08/2026

2.1.2 Experimental Procedure

The crushed GALSs and the clay were characterised to determine their compositions. These samples were then subjected to water absorption, shrinkage, porosity and bulk density as shown in equations 1,2, and 3.

2.1.3 Linear shrinkage.

The lengths (mm) of the different rectangular samples were measured when wet (mould dimension, 90mm x 14mm x 7mm), dried and after firing. The dry, fired, and total shrinkages were determined as follows:

$$\text{Dry shrinkage} = \frac{L_w - L_d}{L_d} \, x \, 100 \quad (1)$$

$$\text{Fired shrinkage} = \frac{L_d - L_f}{L_d} \, x \, 100 \quad (2)$$

$$\text{Total shrinkage} = \frac{L_w - L_f}{L_d} \, x \, 100 \quad (3)$$

Where:

L_d = Dry length (oven dried at 250^{o}C)
L_w = wet length (90mm in this case)
L_f = Fired length (fired at the chosen temp ^{o}C)

The results were then recorded in a table according to the samples used.

2.1.4 Water absorption.

Following firing, the ceramic composite specimens were subjected to water absorption testing in accordance with [28]. The samples were first boiled in water at 100°C for a duration of 2 hours to ensure thorough exposure to thermal and moisture conditions. Subsequently, they were allowed to soak in the same water for an additional 4 hours to facilitate maximum absorption.

The degree of water absorption was determined gravimetrically as a function of the difference in specimen weight before and after immersion. The calculation was performed using the standard equation in (4):

$$\text{Water absorption} = \frac{w_s - w_d}{w_d} \, x \, 100 \quad (4)$$

Where:

w_s = weight of soaked sample after boiling (soaked weight, gm)
w_d = weight of dried sample (dry weight, gm)

This procedure ensured that the samples absorbed adequate water, thereby allowing accurate evaluation of porosity and densification behavior as influenced by firing temperature and composite composition.

2.1.5 Porosity

The boiled and soaked samples were also used for the porosity tests. The samples were suspended from the beam of a balance on a vessel of water, completely submerged or immersed in the water, and the weight (gm) was measured as suspended weight (w_{sp}). The porosity was then calculated as follows in equation 5:

$$\text{Porosity (P)} = \frac{w_s - w_d}{w_s - w_{sp}} \, x \, 100 \quad (5)$$

Where:

w_s = soaked weight (gm)
w_d = dry weight (gm)
w_{sp} = suspended immersed weight (gm)

The porosities of the different samples were recorded according to the firing temperatures.

2.1.6 Bulk density

The dry, soaked and suspended immersed weights of the samples (w_d, w_s and w_{sp}, respectively) were used to determine the bulk densities of the samples according to the direct volume measurements method (the Bulk Density of a brick by water displacement method, the bulk density was calculated as [29] shown in Equation 6:

$$\text{Bulk Density } (\varrho) = \frac{w_d}{w_s - w_{sp}} \, x \, Density \, of \, water \, (\text{Kg/m}^3) \quad (6)$$

Where:

w_s = soaked weight (gm)
w_d = dry weight (gm)
w_{sp} = suspended immersed weight (gm)

Received: 28/08/2026; Revised: 29/08/2026; Accepted: 31/08/2026; Published: 31/08/2026

The calculated bulk densities of the different samples were then tabulated as a function of their firing temperatures.

3.0 Results and Discussion

Table 3 presents the elemental composition of the crushed GALS shells. The analysis revealed carbon, oxygen, and calcium as the predominant constituents, confirming that the shells are primarily composed of calcium carbonate ($CaCO_3$).

Figure 5 illustrates the Scanning Electron Microscopy (SEM) spectrum of the crushed GALS particles, further validating the presence of these elements. The SEM analysis provided microstructural evidence of the distribution of calcium carbonate phases, which are critical in influencing densification, shrinkage, and porosity during firing. The confirmation of $CaCO_3$ as the dominant phase aligns with previous studies on biomineralized shells and supports the hypothesis that the incorporation of GALS shells into clay matrices can enhance ceramic properties through controlled phase transformations at elevated temperatures [30].

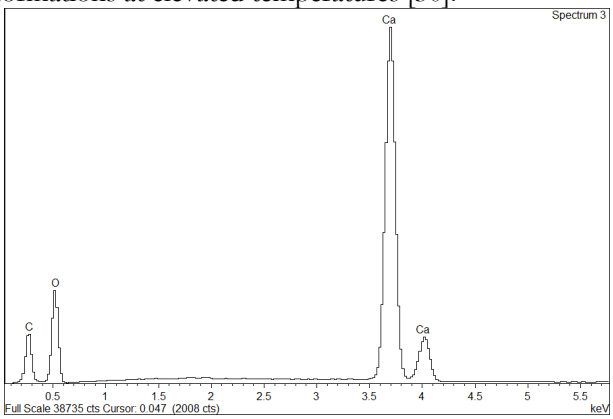

Figure 5: The SEM spectra of the crushed GALS

Table 3: The composition of the crushed GALS

Spectrum	In stats.	C	O	Ca	Total
Spectrum 1	Yes	14.26	52.07	33.66	100.00
Spectrum 2	Yes	14.61	52.91	32.48	100.00
Spectrum 3	Yes	14.00	52.12	33.87	100.00
Mean		14.29	52.37	33.34	100.00
Std. deviation		0.30	0.47	0.75	
Max.		14.61	52.91	33.87	
Min.		14.00	52.07	32.48	

The composition of the clay used is shown in Table 4 indicating oxygen and silica as the main elements. The spectrum from Scanning Electron Microscope (SEM), is shown in Figure 6.

Table 4: The composition of the clay sample

Spectrum	In stats.	C	O	Na	Mg	Al	Si	K	Ca	Ti	Fe	Total
Spectrum 1	Yes	15.29	52.73	0.22	1.22	9.23	16.37	1.42	0.40	0.43	2.69	100.00
Spectrum 2	Yes	16.39	52.12	0.42	1.05	8.40	16.30	1.31	0.59	0.61	2.80	100.00
Spectrum 3	Yes	11.67	55.65	0.14	1.43	9.53	16.72	1.48	0.18	0.49	2.70	100.00
Mean		14.45	53.50	0.26	1.23	9.06	16.47	1.41	0.39	0.51	2.73	100.00
Std. deviation		2.47	1.88	0.14	0.19	0.58	0.22	0.09	0.20	0.09	0.06	
Max.		16.39	55.65	0.42	1.43	9.53	16.72	1.48	0.59	0.61	2.80	
Min.		11.67	52.12	0.14	1.05	8.40	16.30	1.31	0.18	0.43	2.69	

Received: 28/08/2026; Revised: 29/08/2026; Accepted: 31/08/2026; Published: 31/08/2026

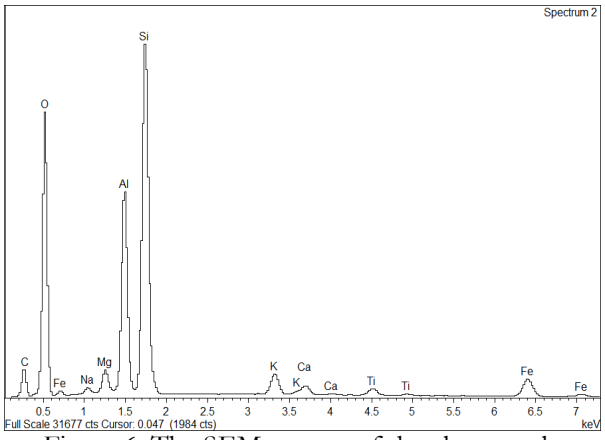

Figure 6: The SEM spectra of the clay sample

Table 6, on the other hand, shows the linear shrinkages only with respect to samples at the specified conditions, that is, the ceramic matrix composite ratios (the particle size of the GALS/clay ratios). Table 5 shows results obtained after the samples were fired and subjected to shrinkage, water absorption, porosity and bulk density tests.

Table 5: The physical properties of the samples

S/N	Sample	Dry Shrinkage, %	Fired Shrinkage, %	Total Shrinkage, %	Water Absorption, %	Porosity, %	Bulk Density, Kg/m³
1	C1001160	4.16	6.20	9.89	6.16	10.14	1640
2	C1001180		5.80	9.50	6.29	6.9	1643
3	C1001200		5.93	9.63	3.65	6.2	1671
4	6310901160	3.87	2.12	5.78	14.55	23.42	1610
5	6310901180		2.00	5.67	15.10	24.38	1614
6	6310901200		1.63	5.30	9.93	17.07	1720
7	6320801160	3.19	0.29	3.47	20.59	33.00	1619
8	6320801180		0.71	3.44	22.22	36.00	1655
9	6320801200		3.85	6.78	4.71	8.16	1735
10	7510901160	3.48	2.10	5.50	15.62	21.30	1567
11	7510901180		2.18	5.58	14.09	24.4	1733
12	7510901200		2.96	6.33	10.60	6.41	1692
13	7520801160	3.28	1.81	4.93	24.90	39.16	1611
14	7520801180		3.40	6.48	25.8	44.1	1752
15	7520801200		4.89	7.91	6.25	8.75	1684

Table 6. The linear shrinkage of the samples

S/N	Sample	Dry Shrinkage %	Fired Shrinkage %	Total Shrinkage %
1	C1001160	4.16	6.20	9.89
2	C1001180		5.80	9.50
3	C1001200		5.93	9.63
4	6310901160	3.87	2.12	5.78
5	6310901180		2.00	5.67
6	6310901200		1.63	5.30
7	6320801160	3.19	0.29	3.47
8	6320801180		0.71	3.44
9	6320801200		3.85	6.78
10	7510901160	3.48	2.10	5.50
11	7510901180		2.18	5.58
12	7510901200		2.96	6.33
13	7520801160	3.28	1.81	4.93
14	7520801180		3.40	6.48
15	7520801200		4.89	7.91

Received: 28/08/2026; Revised: 29/08/2026; Accepted: 31/08/2026; Published: 31/08/2026

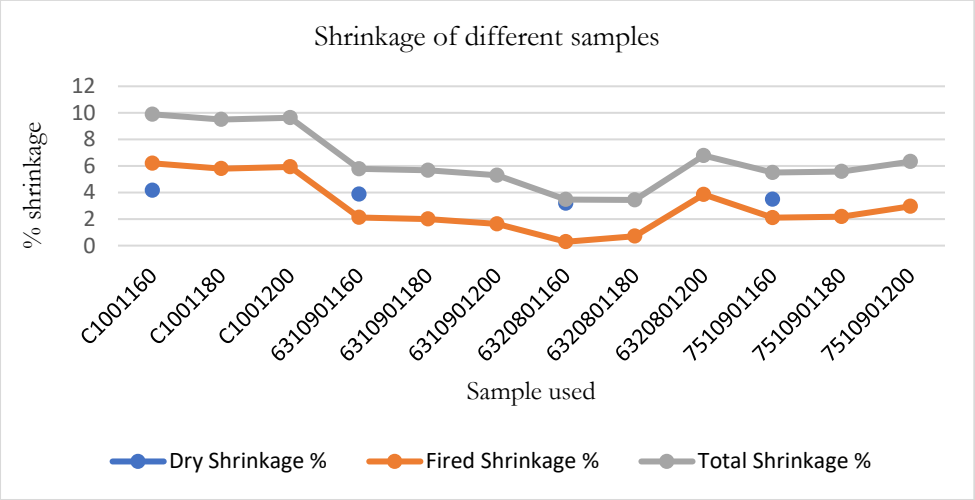

Figure 7: The graph of the percentage shrinkage versus the samples used

Figure 7 above shows the graph of dry shrinkage, fired shrinkage and total shrinkage percentages, from the graph, it could be observed that the reference sample, designated C100, consistently exhibited an excessive shrinkage of approximately >8.0%, which indicates cracking, distortion and dimensional inaccuracy [31]. However, subsequent samples indicate shrinkage values lower than 8% which are within the acceptable limits for ceramic composites [32]. Upon incorporation of (GALS) shell particles into the clay matrix, shrinkage values generally decreased. This reduction can be attributed to the thermal decomposition of calcium carbonate ($CaCO_3$) into calcium oxide (CaO), which modifies the densification pathway of the composite and mitigates excessive contraction.

Overall, shrinkage tended to decrease with increasing firing temperature, reflecting enhanced densification and improved microstructural consolidation at elevated thermal regimes. However, this trend was not uniform across all compositions and was influenced by both the weight percentage and particle size of the GALS inclusions. At 1200°C, samples 6320801200 and 7520801200 demonstrated relatively higher shrinkage values compared to other composites. The elevated shrinkage observed at this temperature is indicative of intensified densification, resulting in stronger interparticle bonding and improved structural integrity of the ceramic matrix [33].

These findings highlight the potential dual role of GALS shell particles: while their decomposition contributes to shrinkage control at moderate firing temperatures, their interaction with the clay matrix at higher temperatures promotes densification, thereby enhancing mechanical stability and suitability for high-voltage insulator applications [34].

Table 7 presents the influence of firing temperature on the water absorption, porosity, and bulk density of the prepared ceramic composites. The data reveal a clear correlation between increasing firing temperature and improved densification behavior. Specifically, water absorption and porosity values decreased progressively with higher firing temperatures, reflecting the reduction of open pores and enhanced consolidation of the matrix. Conversely, bulk density increased with firing temperature, indicating the formation of a more compact microstructure.

Table 7: The effect of firing temperatures on water absorption, porosity, and bulk density of the samples.

S/N	Sample	Water Absorption (%)	Porosity (%)	Bulk Density (kg/m^3)
1	C1001160	6.16	10.14	1640
2	C1001180	6.29	6.9	1643
3	C1001200	3.65	6.2	1671
4	6310901160	14.55	23.42	1610
5	6310901180	15.10	24.38	1614
6	6310901200	9.93	17.07	1720
7	6320801160	20.59	33.00	1619
8	6320801180	22.22	36.00	1655
9	6320801200	4.71	8.16	1735
10	7510901160	15.62	21.30	1567
11	7510901180	14.09	24.4	1733
12	7510901200	10.60	6.41	1692

Received: 28/08/2026; Revised: 29/08/2026; Accepted: 31/08/2026; Published: 31/08/2026

S/N	Sample	Water Absorption (%)	Porosity (%)	Bulk Density (kg/m³)
13	7520801160	24.90	39.16	1611
14	7520801180	25.8	44.1	1752
15	7520801200	6.25	8.75	1684

Figure 8 illustrates the relationship between water absorption and porosity across the different sample compositions. The graphical trend confirms that both properties diminish as firing temperature rises, consistent with the onset of vitrification and glassy phase formation at elevated temperatures. Figure 9 further demonstrates the corresponding increase in bulk density, highlighting the role of GALS shell inclusions in promoting densification relative to the control sample (C100).

This study showcases the effectiveness of incorporating GALS particles into clay matrices, as the composites exhibited superior densification and reduced porosity compared to pure clay. The results suggest that firing at 1200°C yields optimal physical properties, positioning the GALS clay composites as promising candidates for high-voltage insulator applications.

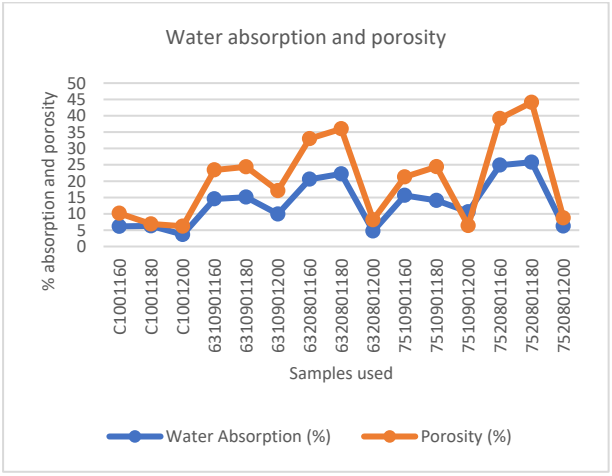

Figure 8: The graph of water absorption and porosity against the samples used

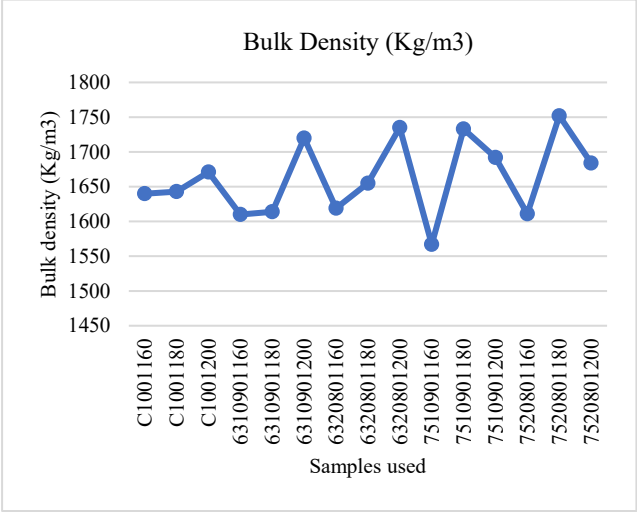

Figure 9: The graph of Bulk density against the samples used

As illustrated in Figure 8, the water absorption and porosity of the ceramic composites initially increased with firing temperature but exhibited a pronounced decline at 1200 °C. This behaviour reflects the onset of significant densification, whereby the microstructure becomes more compact and interconnected pores are effectively eliminated. The reduction in water absorption at this stage is particularly advantageous for electrical applications, as it enhances electrical resistance and ensures reliable insulation performance. Similarly, the decrease in porosity implies improved fracture resistance, supporting the maintenance of dielectric strength and stable insulation properties under service conditions.

Received: 28/08/2026; Revised: 29/08/2026; Accepted: 31/08/2026; Published: 31/08/2026

Figure 9 presents the variation of bulk density with firing temperature. Bulk density, which serves as an indicator of compaction and mechanical integrity, is inversely related to porosity and water absorption. The observed increase in bulk density across all sample sets with rising firing temperature signifies stronger interparticle bonding and reduced void content, thereby imparting greater toughness and impact resistance. Notably, samples 6310901200 and 6320801200 attained the highest bulk density values at 1200 °C, corroborating the densification trend observed in Figure 8.

The results clearly illustrate the enhanced mechanical performance achieved under this firing condition, emphasizing the pivotal influence of GALS shell inclusions in strengthening both the structural integrity and functional characteristics of the composites.

Taken together, the findings confirm that sintering at 1200 °C produces optimal physical properties namely, low water absorption, reduced porosity, and elevated bulk density, thereby establishing GALS clay composites as strong contenders for application in high-voltage electrical insulators.

4.0 Conclusion

This study examined the influence of firing temperature on the physical properties of ceramic matrix composites produced from mixtures of crushed GALS shells and clay. The composites were prepared at varying ratios and particle sizes, then fired at 1160 °C, 1180 °C, and 1200 °C. The specimens were characterized in terms of shrinkage, water absorption, porosity, and bulk density.

The results demonstrated that firing temperature plays a decisive role in determining composite performance. At 1200 °C, all samples exhibited markedly reduced water absorption and porosity, accompanied by increased bulk density, reflecting significant densification and improved microstructural integrity. These changes are particularly advantageous for electrical applications, as low water absorption enhances electrical resistance, while reduced porosity supports fracture resistance and dielectric stability. The increase in bulk density further indicates stronger interparticle bonding and improved mechanical toughness.

Overall, the findings confirm that GALS–clay composites fired at 1200 °C possess the requisite physical properties for high-voltage ceramic insulators. Beyond their functional suitability, the use of GALS shells offers an environmentally beneficial pathway by valorising biological waste and mitigating ecological challenges. This work therefore contributes to both sustainable materials development and the advancement of ceramic technologies for electrical insulation.

Acknowledgement

Faculty of Engineering, University of Abuja, provided facilities to prepare and crush the snail shells before transporting them to Dublin. Department of Mechanical, Manufacturing and Biomedical Engineering, Trinity College Dublin, The University of Dublin, where all the experiments and tests were carried out. TETFUND; provided the funds.

References

[1] Hobson M., *The Wonder of Seashells: Discover the Meaning & Magic of the Ocean's Treasures*. Wellfleet, 2025.

[2] O. L. Adepitan, O. O. Alabi, O. J. Gbadeyan, N. Deenadayalu, and A. T. Jayeola, "Investigation into the development and utilization of snail shell biomaterials: A systematic review," *Discov. Mater.*, vol. 5, no. 1, p. 47, 2025.

[3] N. T. H. Nhung, V. D. Long, and T. Fujita, "A critical review of snail shell material modification for applications in wastewater treatment," *Materials*, vol. 16, no. 3, p. 1095, 2023.

[4] F. Tiwari, "Ecofriendly management of giant African snail (GAS) Achatina fulica (Bowdich)," *Nutrition and Food Processing*, 2024.

[5] I. O. Oladele, L. Onuh, A. S. Taiwo, S. Borisade, N. I. Agbeboh, and S. S. Lephuthing, "Mechanical, wear and thermal conductivity characteristics of snail shell-derived hydroxyapatite reinforced epoxy bio-composites for adhesive biomaterials applications," *International journal of sustainable engineering*, vol. 15, no. 1, pp. 122–135, 2022.

[6] H. Sun, B. Zou, X. Wang, W. Chen, G. Zhang, T. Quan, & C. Huang. Advancements in multi-material additive manufacturing of advanced ceramics: A review of strategies, techniques and equipment. *Materials Chemistry and Physics*, *319*, 129337, 2024.

[7] J. Kim, J. H. Ha, J. Lee, and I. H. Song, "Effect of pore structure on gas permeability constants of porous alumina," *Ceram. Int.*, vol. 45, no. 5, pp. 5231–5239, 2019.

[8] M. A. Ajayi, D. O. Bichang'a, I. O. Oladele, A. O. Alabi, S. A. Oyegunna, and A. F. Ojo, "Analytical evaluation of snail shell derived-nanoparticles/wood ash/charcoal hybrid reinforced epoxy bio-composites," *Discover Polymers*, vol. 3, no. 1, p. 5, 2026.

[9] A. M. Maglad, M. A. O. Mydin, S. D. Datta, and B. A. Tayeh, "Assessing the mechanical, durability, thermal and microstructural properties of sea shell ash based lightweight foamed concrete," *Constr. Build. Mater.*, vol. 402, p. 133018, 2023.

[10] Z. Han, J. Li, H. Wang, and J. Zhao, "Initiation and propagation of a single internal 3D crack in brittle material under dynamic loads," *Eng. Fract. Mech.*, vol. 285, p. 109299, 2023.

[11] H. M. ElSayed, S.A. Yousief, S. Alanazi, M.H. Alyami, A.N.M. Emam, M.N. Alshammari, & M.F. Metwally. Stress Distribution of Hybrid Ceramic Implant-supported Superstructure Versus Zirconia and Lithium Disilicate Superstructures. *The Open Dentistry Journal*, *20*(1), 2026.

[12] A. Nurudeen, I. Dagwa, B. Ugheoke, I. Muhammad, and A. Arogundade, "Effect of magnesia additive on the morphology and physico-mechanical properties of kaolinitic clays ceramics," *Applied Research*, p. e2400053, 2024.

[13] A. Pountouenchi, E.J.A. Ndzana, I.C. Mountapbeme, S. Njuhou, A. Njoya, N. Fagel, & J.A. Mbey. Porous refractory ceramics using agrowastes and some kaolinitic clays. *Open Ceramics*, *18*, 100568. (2024.

[14] E. Gasparini, S.C. Tarantino, G.M.P. Riccardi, I.C. Erika, C. Siligardi, and M. Zema. "Thermal dehydroxylation of kaolinite under isothermal conditions." *Applied Clay Science* 80, p. 417-425. 2013.

[15] B. Amrane, E. Ouedraogo, B. Mamen, S. Djaknoun, and N. Mesrati, "Experimental study of the thermo-mechanical behaviour of alumina-silicate refractory materials based on a mixture of Algerian kaolinitic clays," *Ceram. Int.*, vol. 37, no. 8, pp. 3217–3227, 2011.

[16] A. A. Ayalew, "Physiochemical Characterization of Ethiopian Mined Kaolin Clay through Beneficiation Process," *Advances in Materials Science and Engineering*, vol. 2023, pp. 1–8, 2023.

[17] H. Cheng, Y. Zhou, and Q. Liu, "Kaolinite Nanomaterials: Preparation, Properties and Functional Applications," *Nanomaterials from Clay Minerals: A New Approach to Green Functional Materials*, pp. 285–334, 2019.

[18] F. Yang, C. Li, Y. Lin, and C. A. Wang, "Effects of sintering temperature on properties of porous mullite/corundum ceramics," *Mater. Lett.*, vol. 73, pp. 36–39, 2012.

[19] V. Fuertes, J. J. Reinosa, J. F. Fernández, and E. Enríquez, "Engineered feldspar-based ceramics: A review of their potential in ceramic industry," *J. Eur. Ceram. Soc.*, vol. 42, no. 2, pp. 307–326, 2022.

[20] Li, H., Wang, W., Xu, J., Wang, A., Wan, X., Yang, L., ... & Wang, W. Mn-Based mullites for environmental and energy applications. *Advanced Materials*, *36*(21), p.2312685, 2024.

[21] H. Takada, A. Nakahira, K. Niihara, H. Ohnishi, and K. Toshio, "Fabrication and Evaluation of Natural Mullite Composites," *Journal of The Japan Society of Powder and Powder Metallurgy*, vol. 37, p. 1060–1062, 1990,

[22] R. M. Andrade, A.J. Araújo, R.A. Raimundo, R.P. Dutra, L.F. Campos, C.A. Vivacqua, & D.A. Macedo. Understanding the processing of mullite-based ceramics from kaolin waste: a cautionary note on the inadvertent use of split-plot designs. *Journal of the Australian Ceramic Society*, *61*(2), p. 699-710, 2025.

[23] P. J. Sánchez-Soto, D. Eliche-Quesada, S. Martínez-Martínez, L. Pérez-Villarejo, and E. G. Garzón, "Study of a Waste Kaolin as Raw Material for Mullite Ceramics and Mullite Refractories by Reaction Sintering," *Materials*, vol. 15, p. 583, 2022,

[24] M. Alima, Y. Taibi, K. Labiod, S. Ladjama, S. Benayache, and A. Azzi, "Structural Transformation of Porcelain Insulators using Raw Materials," *Glass Physics and Chemistry*, vol. 51, p. 443–456, 2025.

[25] G. N. Matthew, "Experimental characterization of sustainable biogenic composites reinforced with micro-scale snail shell particles for non-structural applications," *Discov. Mater.*, p.1-17, 2026,

[26] M. El Masloumi, O. Nassiri, A. El Abbassi, H. El Ghouate, and M. Belaqziz, "Development of ecoefficient composite bricks from river sediments and snail shell waste," *Discover Environment*, vol. 3, no. 1, p. 263, 2025.

[27] A. O. Ademola, I. O. Oladele, D. O. Oluyemi, S. R. Oke, I. Akinbamiyorin, and A. S. Taiwo, "Development of polyvinyl chloride composites with enhanced mechanical properties using modified ceramic particles," *Iranian Polymer Journal*, vol. 34, pp. 1425–1434, 2025.

[28] Y. Bu, R. Spragg, and W. J. Weiss, "Comparison of the Pore Volume in Concrete as Determined Using ASTM C642 and Vacuum Saturation," *Adv. Civ. Eng. Mater.*, vol. 3, p. 20130090, 2014.

[29] G. R. Blake and K. H. Hartge, "Bulk Density," *SSSA Book Series*, 2018,

[30] B. Bhattacharyya, P. P. G. Das, S. Borkataki, and R. Boruah, "Microstructural and Elemental Characterization of Mucin and Shell Powder of Giant African Snail, & Lissachatina; (Stylommatophora: Achatinidae)," *HEXAPODA*, pp. 71–79, 2026.

[31] M. Weiß, J. Maurath, N. Willenbacher, and E. Koos, "Shrinkage and dimensional accuracy of porous ceramics derived from capillary suspensions," *J. Eur. Ceram. Soc.*, vol. 39, no. 5, pp. 1887–1892, 2019,

[32] D. Hao, T. Akatsu, N. Kamochi, M. Inada, and A. Shiraishi, "Near-zero sintering shrinkage in pottery with wollastonite addition," *J. Eur. Ceram. Soc.*, vol. 43, no. 2, pp. 700–707, 2023.

Received: 28/08/2026; Revised: 29/08/2026; Accepted: 31/08/2026; Published: 31/08/2026

[33] A. E. Alves, P. L. Bernardo, T. C. Cordeiro, R. da T. Faria, and J. N. F. de Holanda, "Sustainable Seashell Waste-Derived Calcium Niobate: Structural, Morphological, and Thermophysical Properties," *Solids*, vol. 7, no. 4, p. 40, 2026.

[34] C.E. Daniel and B.Z Ogoro, "Composite Additive: Enhancement of Porcelain Insulator Properties using African Giant Land Snail (Archachatina Marginata) Shell," *International Journal of Applied and Advanced Engineering Research*, vol 3, no. 5, p.63-80, 2026.

Received: 28/08/2026; Revised: 29/08/2026; Accepted: 31/08/2026; Published: 31/08/2026